

Quantification of Retinal Transneuronal Degeneration in Human Glaucoma: A Novel Multiphoton-DAPI Approach

Yuan Lei,^{1,2} Nigel Garraban,³ Boris Hermann,¹ David L. Becker,² M. Rosario Hernandez,⁴ Michael E. Boulton,⁵ and James E. Morgan¹

PURPOSE. Glaucoma is presumed to result in the selective loss of retinal ganglion cells. In many neural systems, this loss would initiate a cascade of transneuronal degeneration. The quantification of changes in neuronal populations in the middle layers of the retina can be difficult with conventional histologic techniques. A method was developed based on multiphoton imaging of 4',6'-diamino-2-phenylindole (DAPI)-stained tissue to quantify neuron loss in postmortem human glaucomatous retinas.

METHODS. Retinas from normal and glaucomatous eyes fixed in 4% paraformaldehyde were incubated at 4°C overnight in DAPI solution. DAPI-labeled neurons at different levels of the retina were imaged by multiphoton confocal microscopy. Algorithms were developed for the automated identification of neurons in the retinal ganglion cell layer (RGCL), inner nucleus layer (INL), and outer nuclear layer (ONL).

RESULTS. In glaucomatous retinas, the mean density of RGCs within 4 mm eccentricity was reduced by approximately 45%, with the greatest RGC loss occurring in a region that corresponds to the central 6° to 14° of vision. Significant neuron loss in the INL and ONL was also seen at 2 to 4 mm and 2 to 3 mm eccentricities, respectively. The ratios of neuron densities in the INL and ONL relative to the RGCL (INL/RGC and ONL/RGC, respectively) were found to increase significantly at 3 to 4 mm eccentricity.

CONCLUSIONS. The data confirm that the greatest neuronal loss occurs in the RGCL in human glaucoma. Neuronal loss was also observed in the outer retinal layers (INL and ONL) that correlated spatially with changes in the RGCL. Further work is necessary to confirm whether these changes arise from trans-

neuronal degeneration. (*Invest Ophthalmol Vis Sci.* 2008;49:1940-1945) DOI:10.1167/iov.07-0735

The loss of retinal ganglion cells (RGCs) is a key pathologic event in glaucoma but the extent to which outer retinal layers are affected remains controversial. In human and experimental glaucoma models, histologic evidence supports neuron loss in other layers of the retina outside the retinal ganglion cell layer (RGCL), including the loss of horizontal cells,¹ amacrine cells,²⁻⁴ and the associated thinning of the inner nuclear layer (INL).^{5,6} Swelling and loss of photoreceptors has also been reported in patients with high IOP and end-stage glaucoma.^{7,8} Consistent with these observations, clinical investigations have shown reduced color sensitivity (particularly in the blue-yellow axis) in human glaucoma⁹; in the monkey glaucoma model, aberrant multifocal electroretinography (mfERG) responses were seen in both the inner and outer retina¹⁰; in DBA2 mice, thinning of the outer retinal layers correlated with a decrease in ERG a- and b-wave amplitudes.¹¹ The processes that underlie neuronal loss in the outer retina remain unclear. It is possible that they reflect diffuse retinal damage due to the effect of pressure or retinal ischemia. An alternative explanation is that the outer retinal damage results from transneuronal degeneration secondary to the loss of RGCs, in which case a gradient of neural damage (greatest in the inner retina and least in the outer retina) might be expected. Detailed analysis of the changes in the neuron populations throughout the retina in glaucoma is needed to differentiate these possibilities.

Although significant advances have been made in improving our understanding of retinal neuron topography in human eyes,^{12,13} the detection of transneuronal retinal damage is problematic with conventional imaging techniques such as Nomarski differential interference contrast (NDIC) optics and single-photon confocal microscopy. In the present study, multiphoton confocal microscopy was used to image DAPI labeled neurons (multiphoton-DAPI method) at defined levels of the retina. In multiphoton confocal microscopy, there is near-simultaneous absorption of multiple photons resulting in the emission of a longer-wavelength light that scatters less and has a better tissue penetration.¹⁴ In addition, the imaging plane is restricted to a small diffraction-limited focal volume that allows accurate and high-resolution optical dissection of the retinal wholemount preparations. With the multiphoton-DAPI approach, we determined the degree of transretinal degeneration by quantifying cellular changes in the RGCL, the INL and the outer nuclear layer (ONL) in normal and glaucomatous human retinas.

MATERIAL AND METHODS

Retinal Wholemount Preparation

Eyes were retrieved in accordance with the institutional ethics approval of the Mayo Clinic and University of Washington, St. Louis, and

From the ¹Department of Optometry and Vision Sciences, Cardiff University, Cardiff, United Kingdom; the ²Department of Anatomy and Developmental Biology, University College London, London, United Kingdom; the ³Department of Pathology, University Hospital Wales, Cardiff, United Kingdom; the ⁴Department of Ophthalmology, Northwestern University, Chicago, Illinois; and the ⁵Department of Ophthalmology and Visual Sciences, University of Texas Medical Branch, Galveston, Texas.

Presented at the annual meeting of the Association for Research in Vision and Ophthalmology, Fort Lauderdale, Florida, May 2007.

Supported by Research into Ageing Grant 127.

Submitted for publication June 16, 2007; revised July 20, 2007, and January 3, 2008; accepted March 24, 2008.

Disclosure: **Y. Lei**, None; **N. Garraban**, None; **B. Hermann**, None; **D.L. Becker**, None; **M.R. Hernandez**, None; **M.E. Boulton**, None; **J.E. Morgan**, None

The publication costs of this article were defrayed in part by page charge payment. This article must therefore be marked "advertisement" in accordance with 18 U.S.C. §1734 solely to indicate this fact.

Corresponding author: James E. Morgan, School of Optometry and Vision Sciences, Cardiff University, Cardiff CF24 4LU, UK; morganje3@cardiff.ac.uk.

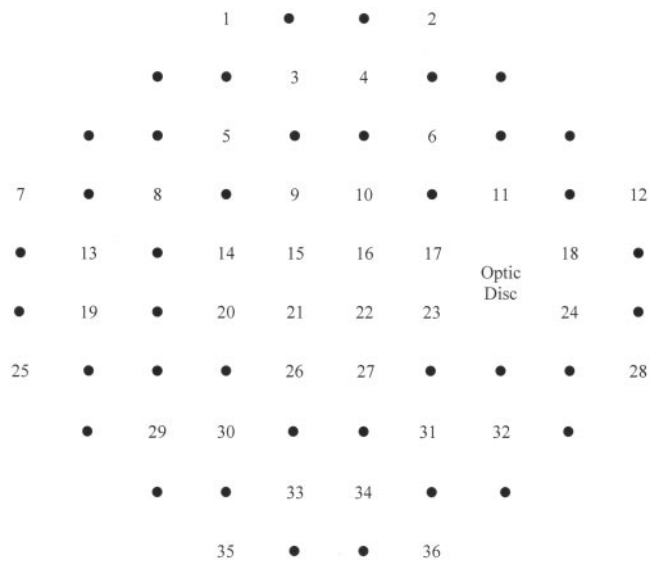


FIGURE 1. Sampling grid used to quantify neuron populations in the RGCL, INL, and ONL of the retina. Sample points correspond retinotopically to the test locations in a Humphrey 30-2 visual field (Carl Zeiss Meditec, Oberkochen, Germany). The fovea was aligned with the center of the grid, which was used with optic disc as reference points in sampling. Points on the grid were 1.7 mm apart (equivalent to 6° eccentricity). Thirty-six numbered points were selected to collect data, and unnumbered locations were not sampled.

the Declaration of Helsinki for research involving human tissue. Six glaucomatous retinas (61–90 years old) and six age-matched control retinas (67–83 years old) were used in the study. Detailed clinical histories were available for the glaucomatous eyes, all of which had primary open-angle glaucoma (POAG) with IOPs before treatment in the range of 20 to 30 mm Hg. Although the clinical histories of control eyes were not available, none was from a patient receiving ophthalmic

care. In all cases, age, gender, ethnic origin, and the cause of death were known. All postmortem human retinas were fixed in 4% paraformaldehyde within 24 hours of death. After the anterior segment and vitreous humor were removed, the retinas were freed from the retinal pigment epithelium. Four equal cuts were made in each retina to yield four approximately equal segments.

Multiphoton-DAPI Imaging

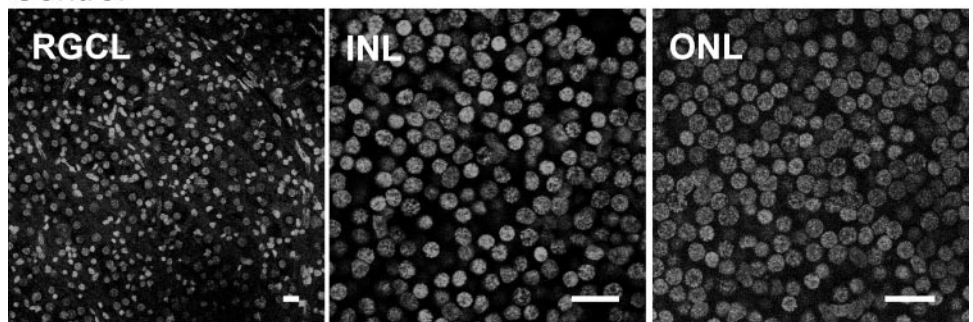
Retinas were stained by DAPI (4,6 diamidino-2-phenylindole; Sigma-Aldrich, Poole, UK) solution (3 $\mu\text{g}/\text{mL}$ in PBS) overnight at 4°C and wholemounted with the RGC side uppermost in a hard-set mounting medium for fluorescence (Vectashield; Vector Laboratories, Burlingame, CA). The specimen was placed on a motorized microscope stage that allowed the selection of any retinal location to an accuracy of 1 μm . DAPI molecules were excited with a Ti:Sapphire multiphoton laser at 843 nm (Tsunami; Newport SpectraPhysics GmbH, Darmstadt, Germany), and images were acquired (model TCS SP2; Leica, Milton Keynes, UK) with a confocal system (DMRE microscope with HCX PL Apo 40/1.25 NA oil CS objective lens; Leica). Laser power, gain, offset, and pinhole size of the confocal microscope were kept constant at each session, to facilitate comparisons between retinas.

To relate retinal disease to clinical data, a sampling grid, which retinotopically corresponded to the spacing stimuli in a 30-2 visual field analyser (Humphrey; Carl Zeiss Meditec, Oberkochen Germany) was used to define sample locations (Fig. 1).^{15,16} To correlate anatomic positions on the retina to visual field, we converted the distance (in millimeters) to degrees of visual angle according to a nonlinear conversion of retinal magnification factor¹⁷ ($y = 0.035x^2 + 3.4x + 0.1$, where y is the eccentricity in arc degrees, and x is in millimeters).

Automated Detection of Cell Nuclei

Neuron nuclei were detected and counted by an established method¹⁸ that was implemented as a plug-in in the public domain of ImageJ (ver. 1.34).¹⁹ In the projected images of each retinal layer, the average

Control



Glaucoma

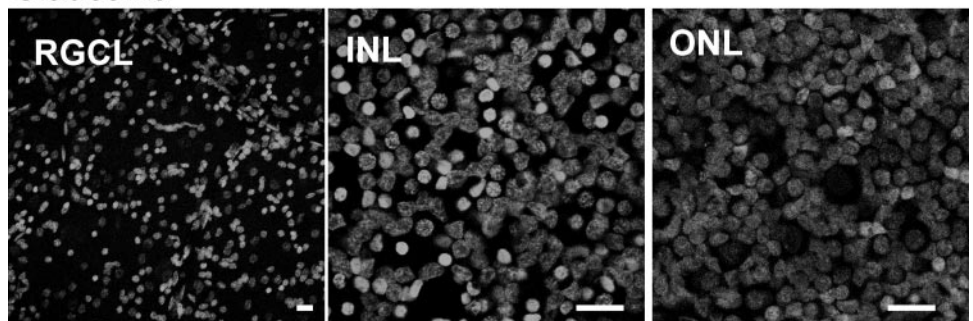


FIGURE 2. Multiphoton projection images of DAPI-stained cell nuclei in the RGCL, INL, and ONL of control and glaucomatous human retinal wholemounts. Neuron densities were measured at the magnification of $\times 400$ for neurons in the RGCL, and $\times 1600$ for the INL and ONL. Each z -plane was 10 μm thick with a 0.5- μm interval between planes. The projection image for any given layer was generated from the sum of the component z -planes. Scale bar, 20 μm .

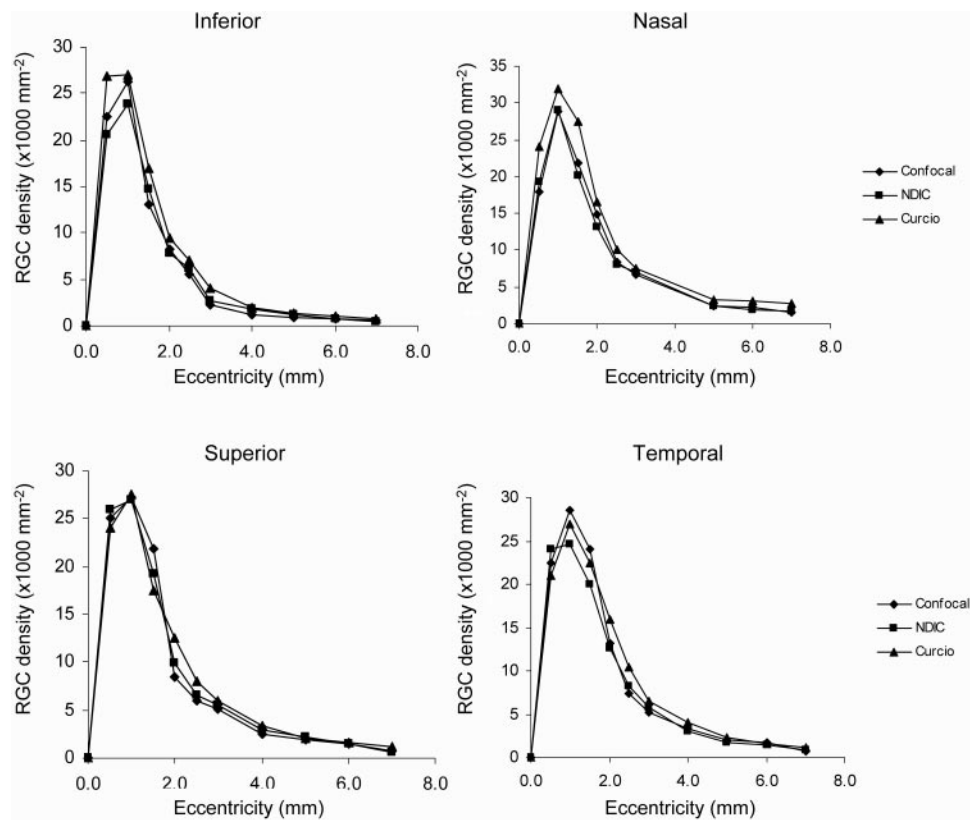


FIGURE 3. Comparisons of RGC quantities measured by the multiphoton-DAPI method ($n = 3$), with NDIC optics ($n = 3$), and literature values ($n = 5$). The measurements were taken at nasal, temporal, superior, and inferior regions of the same retinal wholemounts. Retinas were cleared by DMSO for NDIC imaging.

nuclei diameters were determined, to give the width threshold in pixels. Endothelial cells and glial cells were excluded from counting results by shape and size factors. The multiphoton-DAPI method was validated against the conventional NDIC method¹² by comparing RGC layer counts of the same specimen. The RGCL neuron density was corrected for the presence of displaced amacrine cells, to give RGC densities at different eccentricities of the retina.^{12,13}

Statistics

Statistical analysis was performed with commercial software (SPSS, ver. 14.0 for Windows; SPSS, Chicago, IL). A general linear model was used to compare neuron densities and ratios at different eccentricities of the retina in control and glaucoma groups. For each retinal layer, a repeated-measures analysis was performed with Bonferroni correction. Differences were considered significant at a 95% level of confidence or higher.

RESULTS

At each location of the sampling grid, neurons at the RGCL, INL, and ONL were imaged sequentially; the projected images of each layer are shown in Figure 2 of typical control and glaucomatous retinas. Our estimation of RGC density in the elderly was 70% of that reported for younger adults, which was expected, considering the effect of ageing¹² (Fig. 3).

Neuron Quantification in the RGCL, INL, and ONL

The retinal areas imaged represented 56% of the total area within the central 4-mm eccentricity and 27% between 4- and

7-mm eccentricity. In total, 37,425 neurons were counted in glaucomatous retinas (61-90 years old, $n = 6$) and 57,858 in age-matched control retinas (67-83 years old, $n = 6$). The neuron densities were illustrated by color-coded density maps (Fig. 4). Our data confirmed that RGCL cell density was highest in the perifoveal region; neuron densities in the INL were higher in the peripheral relative to the central retina; the peak density for ONL neurons was at the fovea as expected.

Mean neuron densities in glaucomatous eyes were compared with those in aged-matched control eyes (Fig. 5). In glaucomatous retinas, there were significant reductions of RGCs at all eccentricities tested (Fig. 5A); the mean density of RGCs within 4-mm eccentricity was reduced by approximately 42% (from 13,200–7,700/mm²), with the greatest RGC loss at 2-mm eccentricity (mean \pm SD, 48% \pm 5%). In the INL and ONL, significant reductions of neuron densities were recorded at 2- to 4-mm eccentricity (10%; Fig. 5B; $P < 0.05$) and at 2- to 3-mm eccentricity (7%; Fig. 5C, $P < 0.05$), respectively.

Correlation of Neuron Densities

In view of the variation of neuron densities between retinas, we expressed the relationship of neuron densities in different layers of the retina as ratios (e.g., at a given eccentricity), the INL neurons density divided by the RGCL neuron density (INL/RGCL, Fig. 6). Within the area examined, the ratios of INL to RGCL and ONL to RGCL in glaucomatous retinas were significantly higher than in control retinas between 3 and 4 mm eccentricity ($P < 0.05$, Figs. 6A, 6B). However, there was no

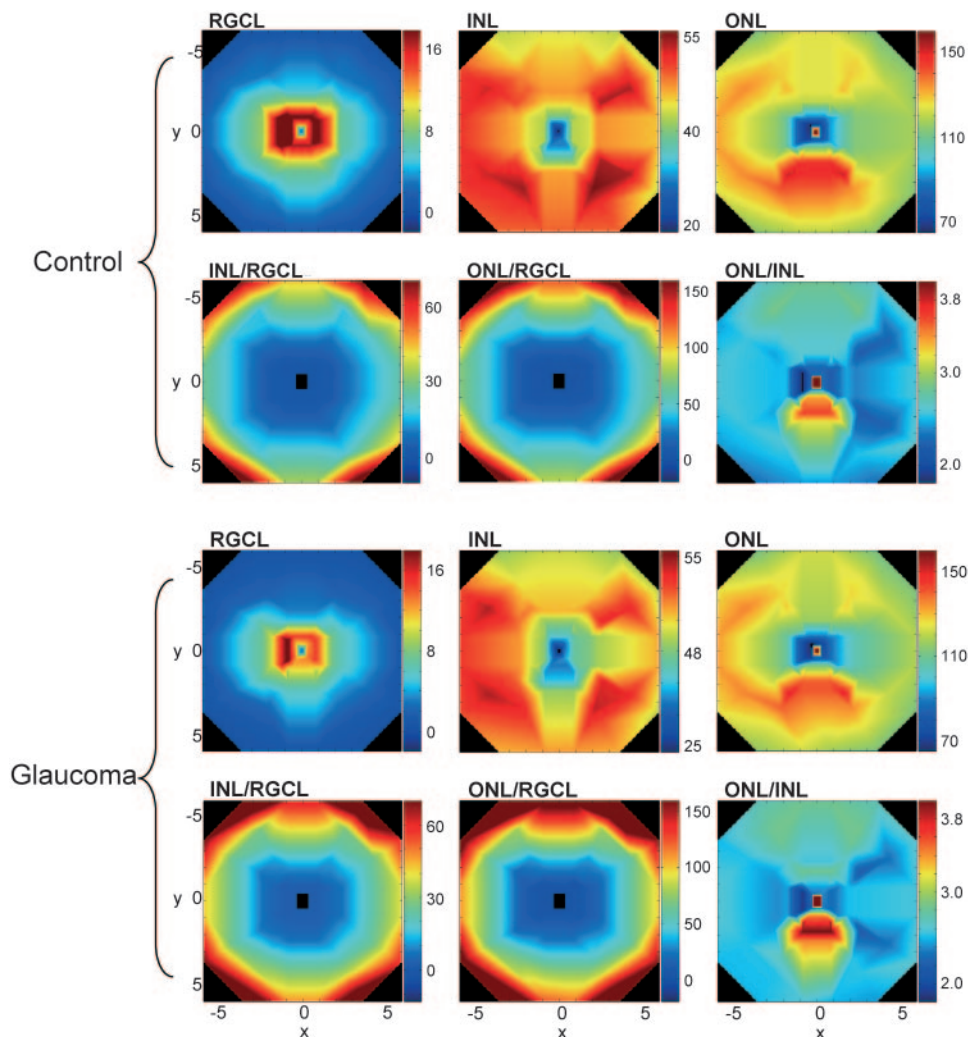


FIGURE 4. Color-coded neuron density maps and correlation maps in control and glaucomatous retinas. The color gradient is assigned to density values and ratios, as shown on the right of each contour plot. Positions on the contour map correlate with those on the sampling grid. Eccentricities are shown on the x and y axes in millimeters, and each map is centered on the fovea.

significant difference in the ONL INL ratio in control and glaucomatous groups at any eccentricity tested (Fig. 6C).

DISCUSSION

The multiphoton-DAPI method allowed us to detect small changes in the neuronal densities in different layers of the retina. This technique revealed cell densities that are similar to those found in previous work taking age into account,^{12,20} (i.e., on average, RGC counts in the central retina of our aged normal eyes; 61–90 years old were 30% less than values published for younger eyes; 27–37 years); the reduction was greatest in the nasal and smallest in the inferior retina. We observed substantial reductions of RGC densities in the glaucomatous retinas, with the greatest percentage loss occurring in a para-central distribution. An important finding is that significant reductions in neuron densities also occurred in the INL (2- to 4-mm eccentricity) and ONL (2- to 3-mm eccentricity) in regions where percentage RGC loss was greatest. Analysis of the relative ratio of neuron densities at a given eccentricity confirms a reduction in both the middle and outer retinal layers.

Our data are consistent with the hypothesis that glaucoma results in damage to the ONL with consequent photoreceptor loss. Previous histologic studies in eyes with open-angle glaucoma have not shown this as a consistent finding. Nork et al.⁷ reported photoreceptor loss in less than 20% of glaucomatous retinas with cone perikaryal swelling occurring in only 25% of those eyes with substantial (>90%) RGC loss. It is interesting to note that the use of more sensitive techniques, such as measurements of red-green and blue cone opsin mRNA, has demonstrated that outer retinal damage is a more consistent feature in primate glaucoma.²¹ In our study, RGC loss was moderate at 42% compared with that in control eyes, and yet we found consistent evidence of outer retinal damage in these eyes. It is likely that our findings reflect the greater sensitivity of the multiphoton-DAPI technique in the quantification of neuronal population throughout a selected retinal volume.

Our observation that the increases in the INL/RGCL and ONL/RGCL ratios in the glaucomatous eyes coincided with the region of the greatest RGC loss (Figs. 5, 6) suggests that RGC loss and outer retinal damage are spatially correlated, and the INL and ONL damage are not simply the result of nonspecific

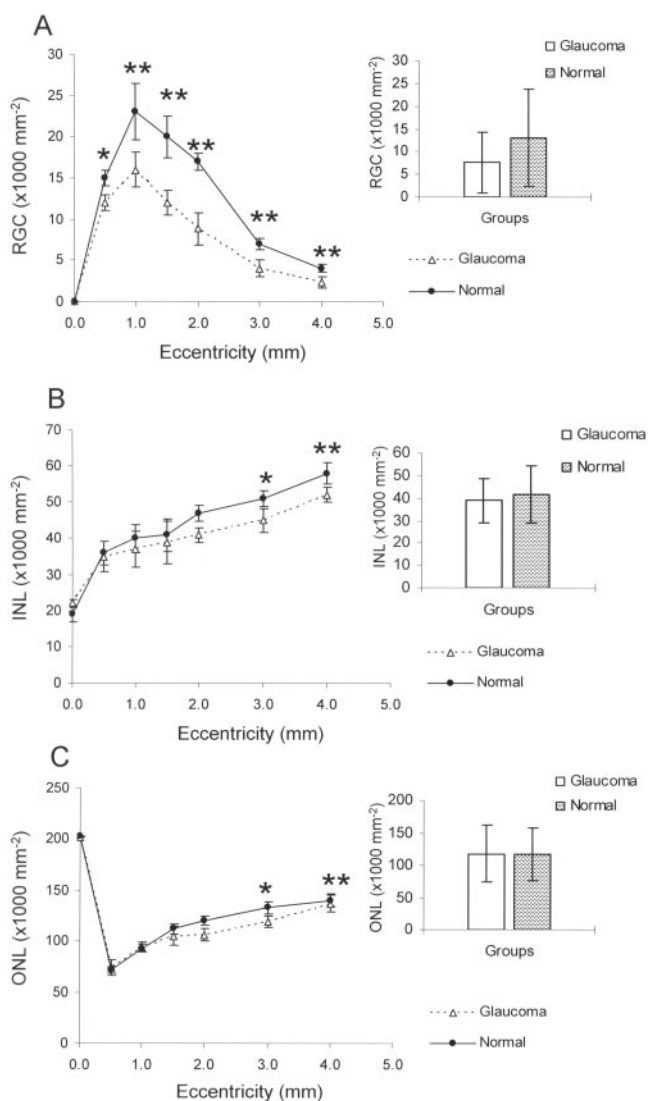


FIGURE 5. Comparisons of neuron densities in the RGCL (A), INL (B), and ONL (C) of glaucomatous ($n = 6$) and control ($n = 6$) retinas. The line graph shows means of neuron densities at each eccentricity, and the histogram shows means within a 4-mm eccentricity. Error bars, ± 1 SD. * $P < 0.05$, ** $P < 0.01$.

retinal damage. Our data cannot confirm that transneuronal effects are responsible for damages in the INL and ONL, but this should be considered as a factor.

The cause of outer retinal damage remains to be clarified. It is possible that it reflects the toxic effect of the release of neurotransmitters such as glutamate. Although it now seems unlikely that this release will result in toxic neurotransmitter levels that can be detected in the vitreous,²² local levels may be elevated to increase the risk of cell loss.²³ The importance of this in the propagation of further cell loss is controversial, since glutamate uptake mechanisms in experimental glaucoma do not appear to be compromised.²⁴ Other factors that may play a role in propagating neuronal loss outside the RGCL layer include the release of free radicals or alterations in the concentration of extracellular calcium.²⁵⁻²⁸ At the level of the RGCL, there is evidence that partial damage to the optic nerve can increase the risk of loss of other adjacent cells as a bystander effect.^{29,30}

Our data highlight the importance of transretinal degeneration in human glaucoma. Because the outer retinal neurons are lost, some of these changes are irreversible, which emphasizes the importance of developing methods for the detection of outer retinal damage.³¹ Neuroprotection in glaucoma is focused on the prevention of RGC loss in ways that complement oculohypotensive treatment. Consideration should also be given to the prevention of outer retinal damage to maximize the efficacy of this approach.

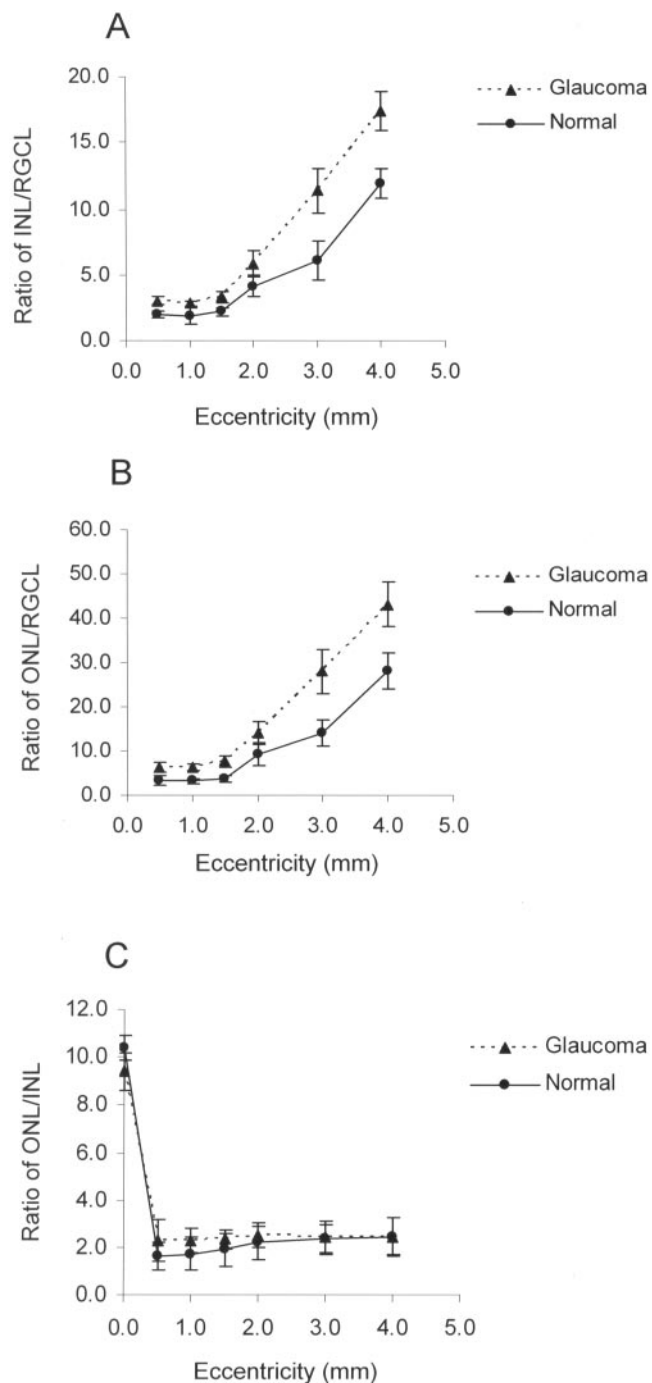


FIGURE 6. Neuron density ratios of INL to RGCL (A), ONL to RGCL (B), and ONL to INL (C) in glaucomatous ($n = 6$) and control ($n = 6$) retinas. Lines show means of neuron density ratios at each eccentricity. Error bars, ± 1 SD.

Acknowledgments

The authors thank Geoff Arden, City University, London, for comments on the manuscript; Christopher Thrasivoulou and Daniel Ciantar for technical support; and Paul McGeoghan for statistical support.

References

- Janssen P, Naskar R, Moore S, Thanos S, Thiel H. Evidence for glaucoma-induced horizontal cell alterations in the human retina. *Ger J Ophthalmol*. 1996;5:378-385.
- May CA, Mittag T. Neuronal nitric oxide synthase (nNOS) positive retinal amacrine cells are altered in the DBA/2NNia mouse, a murine model for angle-closure glaucoma. *J Glaucoma*. 2004;13:496-499.
- Moon JI, Kim IB, Gwon JS, et al. Changes in retinal neuronal populations in the DBA/2J mouse. *Cell Tissue Res*. 2005;320:51-59.
- Wang X, Ng YK, Tay SS. Factors contributing to neuronal degeneration in retinas of experimental glaucomatous rats. *J Neurosci Res*. 2005;82:674-689.
- Dkhissi O, Chanut E, Versaux-Botteri C, et al. Changes in retinal dopaminergic cells and dopamine rhythmic metabolism during the development of a glaucoma-like disorder in quails. *Invest Ophthalmol Vis Sci*. 1996;37:2335-2344.
- Osborne NN, Ugarte M, Chao M, et al. Neuroprotection in relation to retinal ischemia and relevance to glaucoma. *Surv Ophthalmol*. 1999;43(suppl 1):S102-S128.
- Nork TM, Ver Hoeve JN, Poulsen GL, et al. Swelling and loss of photoreceptors in chronic human and experimental glaucomas. *Arch Ophthalmol*. 2000;118:235-245.
- Panda S, Jonas JB. Decreased photoreceptor count in human eyes with secondary angle-closure glaucoma. *Invest Ophthalmol Vis Sci*. 1992;33:2532-2536.
- Nork TM. Acquired color vision loss and a possible mechanism of ganglion cell death in glaucoma. *Trans Am Ophthalmol Soc*. 2000;98:331-363.
- Raz D, Perlman I, Percicot CL, Lambrou GN, Ofri R. Functional damage to inner and outer retinal cells in experimental glaucoma. *Invest Ophthalmol Vis Sci*. 2003;44:3675-3684.
- Bayer AU, Neuhardt T, May AC, et al. Retinal morphology and ERG response in the DBA/2NNia mouse model of angle-closure glaucoma. *Invest Ophthalmol Vis Sci*. 2001;42:1258-1265.
- Curcio CA, Allen KA. Topography of ganglion cells in human retina. *J Comp Neurol*. 1990;300:5-25.
- Curcio CA, Drucker DN. Retinal ganglion cells in Alzheimer's disease and aging. *Ann Neurol*. 1993;33:248-257.
- Tauer U. Advantages and risks of multiphoton microscopy in physiology. *Exp Physiol*. 2002;87:709-714.
- Kerrigan-Baumrind LA, Quigley HA, Pease ME, Kerrigan DF, Mitchell RS. Number of ganglion cells in glaucoma eyes compared with threshold visual field tests in the same persons. *Invest Ophthalmol Vis Sci*. 2000;41:741-748.
- Morgan JE, Uchida H, Caprioli J. Retinal ganglion cell death in experimental glaucoma. *Br J Ophthalmol*. 2000;84:303-310.
- Drasdo N, Fowler CW. Non-linear projection of the retinal image in a wide-angle schematic eye. *Br J Ophthalmol*. 1974;58:709-714.
- Byun J, Verardo MR, Sumengen B, et al. Automated tool for the detection of cell nuclei in digital microscopic images: application to retinal images. *Mol Vis*. 2006;12:949-960.
- Rasband WS. ImageJ, U. S. National Institutes of Health, Bethesda, MD; 1997-2006. Available at <http://rsb.info.nih.gov/ij/>.
- Curcio CA. Photoreceptor topography in ageing and age-related maculopathy. *Eye*. 2001;15:376-383.
- Pelzel HR, Schlamp CL, Poulsen GL, et al. Decrease of cone opsin mRNA in experimental ocular hypertension. *Mol Vis*. 2006;12:1272-1282.
- Honkanen RA, Baruah S, Zimmerman MB, et al. Vitreous amino acid concentrations in patients with glaucoma undergoing vitrectomy. *Arch Ophthalmol*. 2003;121:183-188.
- Carter-Dawson L, Shen FF, Harwerth RS, et al. Glutathione content is altered in Muller cells of monkey eyes with experimental glaucoma. *Neurosci Lett*. 2004;364:7-10.
- Hartwick AT, Zhang X, Chauhan BC, Baldrige WH. Functional assessment of glutamate clearance mechanisms in a chronic rat glaucoma model using retinal ganglion cell calcium imaging. *J Neurochem*. 2005;94:794-807.
- Lipton SA. The molecular basis of memantine action in Alzheimer's disease and other neurologic disorders: low-affinity, uncompetitive antagonism. *Curr Alzheimer Res*. 2005;2:155-165.
- Lin MT, Beal MF. Mitochondrial dysfunction and oxidative stress in neurodegenerative diseases. *Nature*. 2006;443:787-795.
- Levin LA. Relevance of the site of injury of glaucoma to neuroprotective strategies. *Surv Ophthalmol*. 2001;45(suppl 3):S243-S249; discussion S273-S246.
- Nickells RW. From ocular hypertension to ganglion cell death: a theoretical sequence of events leading to glaucoma. *Can J Ophthalmol*. 2007;42:278-287.
- Levkovitch-Verbin H, Quigley HA, Kerrigan-Baumrind LA, et al. Optic nerve transection in monkeys may result in secondary degeneration of retinal ganglion cells. *Invest Ophthalmol Vis Sci*. 2001;42:975-982.
- Levkovitch-Verbin H, Quigley HA, Martin KRG, et al. A model to study differences between primary and secondary degeneration of retinal ganglion cells in rats by partial optic nerve transection. *Invest Ophthalmol Vis Sci*. 2003;44:3388-3393.
- Drasdo N, Aldebasi YH, Chiti Z, et al. The s-cone PHNR and pattern ERG in primary open angle glaucoma. *Invest Ophthalmol Vis Sci*. 2001;42:1266-1272.